Available online at www.sciencedirect.com
SCIENCE DIRECT®
Journal of Power Sources 140 (2005) 311–318
JOURNAL OF POWER SOURCES
www.elsevier.com/locate/jpowsour

Novel gas distributors and optimization for high power density in fuel cells

P.W. Li*, S.P. Chen, M.K. Chyu

Department of Mechanical Engineering, University of Pittsburgh, Pittsburgh, PA 15261, USA

Received 27 July 2004; accepted 20 August 2004
Available online 14 October 2004

Abstract

A novel gas distributor for fuel cells is proposed. It has three-dimensional current-collecting elements distributed in gas-delivery fields for effective current collection and heat/mass transfer enhancement. An analysis model has been developed in order to understand the performance of the output power density when the dimensions and distributive arrangement of the current collectors are different. Optimization analysis for a planar-type SOFC was conducted in order to outline the approach in optimizing a gas-delivery field when adopting three-dimensional current-collecting elements in a fuel cell. Experimental test of a proton exchange membrane (PEM) fuel cell adopting the novel gas distributor was conducted for verification of the new approach. Significant improvement of power output was obtained for the proposed new PEM fuel cells compared to the conventional ones under the same conditions except for the different gas distributors. Both the experimental results and modeling analysis are of great significance to the design of fuel cells of high power density.

Keywords: Novel gas distributors; High power density; Fuel cells; Optimization

1. Introduction

Fuel cells can convert the chemical energy of a fuel directly into electrical power with high efficiency and low level of emission [1,2]. It is very promising that fuel cells will gradually be used as the major power source for portable electronic devices, home appliances, vehicles and transportation tools, and even stationary power plants [3,4].

Having a high power density is one of the critical requirements for a fuel cell or a fuel cell stack. Minimized size and usage of materials are important to the low cost and better mobility of fuel cells, especially when they are used in portable devices and/or transportation tools.

In order to have a high power density, a fuel cell has to maintain a reasonably high terminal voltage and a maximized current output [5]. There are three kinds of polarizations that cause potential losses and low terminal voltage of a fuel cell, including activation polarization, ohmic polarization and concentration polarization. It is well known that when operating current density continues to increase, there is an excessive drop of the cell voltage and further improvement of the fuel cell power becomes impossible [6]. Therefore, if one can postpone the excessive drop of fuel cell voltage at higher current density, the power output of the fuel cell can be significantly improved.

The minimization of the activation polarization mostly relies on the materials of electrolyte, electrodes, as well as the catalyst for electrochemical reaction. The reduction of ohmic polarization relies on higher ionic and electronic conductivity of electrolyte and electrodes as well as on the current-collecting route by the current collectors. The latter can even be more significant, for example, in a tubular-type solid oxide fuel cell (SOFC) compared to a planar-type SOFC [7,8]. The alleviation of the concentration polarization in a fuel cell, however, completely relies on the arrangement of the flow

* Corresponding author. Tel.: +1 412 624 3069; fax: +1 412 624 4846.
E-mail addresses: pel1@engr.pitt.edu (P.W. Li), shc10@pitt.edu (S.P. Chen), mkchyu@engr.pitt.edu (M.K. Chyu).

0378-7753/$ – see front matter © 2004 Elsevier B.V. All rights reserved.
doi:10.1016/j.jpowsour.2004.08.031

Nomenclature

E	cell voltage (V)
EMF	electromotive force (V)
f	a general function
F	Faraday's constant (=96486.7 C mol^{-1})
ΔG^0	standard Gibb's free energy change in formation of water (LHV) from oxygen and hydrogen (J kg^{-1})
i	current density of fuel cell (A m^{-2})
i_0	exchange current density (A m^{-2})
I	current (A)
r	radius (m)
R	universal gas constant (8.314 J (mol K)$^{-1}$)
R_e	resistance (Ω)
T	temperature (K)

Greek symbols

δ	thickness of electrode and electrolyte (m)
η^{Act}	activation polarization (V)
ρ_e	resistivity (Ω m)

Subscripts

c	current collectors
0	current-collecting area of one current collector

Superscripts

a	anode
c	cathode
e	electrolyte

fields of the reactant gases or the delivery and removal of the reactants and product to and from the reaction site, respectively. The investigation in this work will focus on minimizing the ohmic polarization and concentration polarization in order to improve the power density of a fuel cell, which is related to designing and optimization of gas distributors and current collectors.

In a proton exchange membrane (PEM) fuel cell or a planar-type solid oxide fuel cell (SOFC), the anode, electrolyte and cathode are laminated as a tri-layer core component, known as MEA (membrane electrode assembly) for a PEM fuel cell. One fuel cell must have two gas delivery plates engraved with gas channels, one for air or oxygen in contact with cathode and another for fuel in contact with anode. Whereas the reactant/product gases flow through the channels, the channel walls act as current collectors to collect current and transmit it out from the fuel cell. The electrochemical reaction occurs at the surfaces of electrodes or electrodes/electrolyte interfaces that are exposed to reactant gases, while the electrons involved in the electrochemical reaction have to conduct in the in-plane direction of the electrode layers before collection by the channel walls or current collectors. Obviously, for the gas distributors of fuel cells, one has to make a balance to promote mass transfer in gas flow field and reduce the ohmic loss in current collection, and, at the same time, allow maximum surface area of the electrodes to expose to reactant gases for electrochemical reaction. The larger the reaction area, the higher the current in the fuel cell.

2. Development of novel gas distributors and analysis model

2.1. Novel gas distributors

In the current fuel cell technology, the gas-delivery plates of PEM fuel cells and planar-type SOFCs have straight grooves or ditches engraved for gas delivery [9–11]. As shown in Fig. 1, such structures of gas channels are straightforward; however, most of them are not optimized. There is no general knowledge available regarding how to distribute the area of current-collecting walls and gas-delivery channels. In order to improve the output current and power density in a fuel cell, conducting an optimization of gas-delivery channels and gas flow field is very necessary.

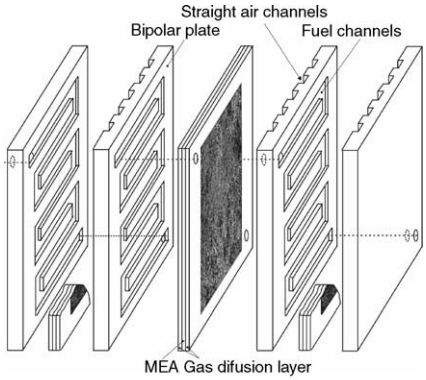

(a) A stack of PEM fuel cells

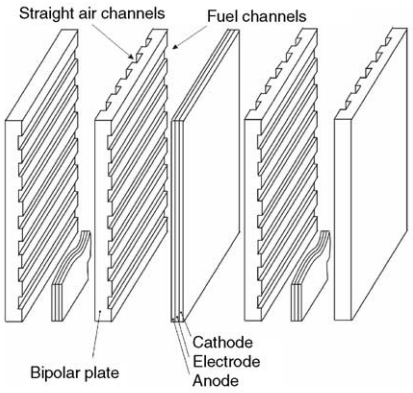

(b) A stack of planar type SOFCs

Fig. 1. Structures of conventional gas channels for fuel cells.

Of many effective heat/mass transfer enhancement approaches, the method that allocates protruding elements in a flow field [12,13] is found to be very suitable to meet the purpose of current collection and mass transfer enhancement in gas flow field for fuel cells. Fig. 2 shows the conceptual protruding elements as current collectors in gas flow fields. For convenience, only cylindrical elements are drawn in the figure, however the geometry of the elements may vary depending on performance and ease of manufacturing of the gas-delivery plate. There are several major advantages of such a gas flow field. First, an MEA or an anode/electrolyte/cathode layer can expose a larger area to the reactant gases when contacting gas-delivery plates. This maximizes the reactive area and is helpful for the fuel cell to obtain larger current. Second, in such a flow field, the gas streams are expected to "communicate" more easily and thus create a more uniform distribution of gases over the reactive surface of the MEA of a PEM fuel cell or the anode/electrolyte/cathode layer of an SOFC. The discrete nature of the protruding elements can promote mixing of the flow stream, which enhances the diffusion of reactant and product to and from the reaction site, respectively. The heat transfer in the flow fields can also be enhanced, which might be critical when the heat generation rate is elevated at high operating current densities.

The novel approach shown in Fig. 2 for gas delivery is expected to be generally advantageous. However, the interruption of the channel walls can result in less contact area of the current collectors to electrodes. Under such a situation, electrons from some area of reaction site have to go a longer way in electrode layers in the in-plane direction before collected by current collectors. If the pathway of electrons is too long in the in-plane direction of electrode layers, a large ohmic loss can result, which can offset the effect of power improvement by maximization of current when using the distributed current collectors in a fuel cell. This needs to find an optimal dimension and distribution of the current collectors in order to obtain a maximum power density. An analysis model for the optimization is, therefore, very necessary.

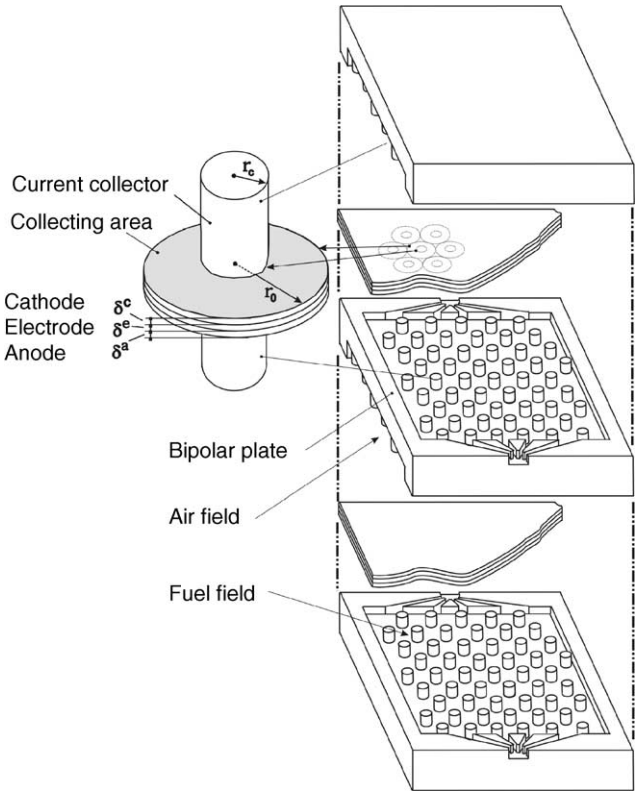

Fig. 2. Protruding current collectors in gas flow fields.

2.2. Model for a fuel cell using novel gas distributors

A magnified schematic view of current collectors on each side of the cathode/electrolyte/anode layer is shown in Fig. 2. The current from the area surrounding the current collector conducts through the in-plane direction of the electrode layers before it is collected. For convenience of analysis, cylindrical current collectors in a staggered alignment are considered. The potential difference between current collectors of the anode side and cathode side is the output voltage of the fuel cell, which is associated to the electromotive force, the dimensions of the current-collecting area, and length of the current pathway in the in-plane direction in electrode layers:

$$E = \mathrm{EMF} - (\eta_{\mathrm{a}}^{\mathrm{Act}} + \eta_{\mathrm{c}}^{\mathrm{Act}}) - R_{\mathrm{e}}^{\mathrm{a}} I - R_{\mathrm{e}}^{\mathrm{c}} I - R_{\mathrm{e}}^{\mathrm{e}} I \tag{1}$$

where E is the output voltage, EMF and η^{Act} are the electromotive force and activation polarization, respectively, and they are also assumed uniform for the control area surrounding the current collector. R_{e} denotes for resistances and I is the current integrated from the control area surrounding the current collector. Considering a current collector of radius r_{c} and a circular control area, or current-collecting area, of radius r_0, the resistances in anode, cathode and electrolyte are:

$$R_{\mathrm{e}}^{\mathrm{a}} = \frac{\rho_{\mathrm{e}}^{\mathrm{a}}((r_0 - r_{\mathrm{c}})/2)}{[\delta^{\mathrm{a}} \cdot 2\pi(r_{\mathrm{c}} + ((r_0 - r_{\mathrm{c}})/2)]} \tag{2a}$$

$$R_{\mathrm{e}}^{\mathrm{c}} = \frac{\rho_{\mathrm{e}}^{\mathrm{c}}((r_0 - r_{\mathrm{c}})/2)}{[\delta^{\mathrm{c}} \cdot 2\pi(r_{\mathrm{c}} + ((r_0 - r_{\mathrm{c}})/2)]} \tag{2b}$$

$$R_{\mathrm{e}}^{\mathrm{e}} = \frac{\rho_{\mathrm{e}}^{\mathrm{e}} \delta^{\mathrm{e}}}{\pi(r_0^2 - r_{\mathrm{c}}^2)} \tag{2c}$$

where $\rho_{\mathrm{e}}^{\mathrm{a}}$, $\rho_{\mathrm{e}}^{\mathrm{c}}$ and $\rho_{\mathrm{e}}^{\mathrm{e}}$ are the resistivities of anode, cathode and electrolyte, respectively, and δ^{a}, δ^{c} and δ^{e} are thickness of anode, cathode and electrolyte layers, respectively.

Assuming that the average current density over the area in radius of r_0 is i, the total current collected by the current collector is

$$I = i \cdot \pi r_0^2 \tag{3}$$

The power density over the area in radius of r_0 is

$$P = \frac{EI}{\pi r_0^2} = f(r_c, i) \quad (4)$$

As a function of the current density and the radius r_c of the cylindrical current collector in the control area in radius of r_0, the power density is qualitatively illustrated in Fig. 3 by the contour. The variation of the contour shows a feature very useful for one to optimize the dimensions of current collectors in order to have a maximum power density.

Virtually, Fig. 3 indicates that a smaller current collector is favorable for getting a higher power density in general. In a fixed area of radius of r_0, the smaller the current collector, the larger area of the layer of anode/electrolyte/cathode can have electrochemical reaction to obtain a larger current for the fuel cell.

On the other hand, the usage of a small current collector can result in longer pathway for a current to flow in the in-plane direction of electrode layers. Therefore, a decrement of the resultant power output due to large ohmic loss happens when a current density is very high, as seen in Fig. 3. There exists an optimal setting of a current collector and its control area.

It is understood from the above analysis that the interruption of the straight gas channel walls can be effective for maximizing the current and power output of a fuel cell. When current density is very high, optimization of the current collector is necessary. To give quantitative analysis, computational results are to be discussed in the next section based on the real property data of an SOFC when three-dimensional protruding elements or distributed current collectors are adopted. For PEM fuel cells, experimental results will be reported in the section following the next.

3. Optimization analysis for a planar-type SOFC

Using protruding elements as current collectors, a planar-type solid oxide fuel cell may have maximized area for reactant gases to access the electrode/electrolyte layer. This can definitely improve the total current for the fuel cell. However, to obtain a maximized benefit from the utilization of the protruding elements as current collectors, optimization analysis for dimensions of the current collectors and their control area is necessary. The dimensions and resistivities of the electrodes and electrolyte of a planar-type SOFC for analysis are given in Table 1 [8] assuming that the SOFC operates at temperature of 1000 °C.

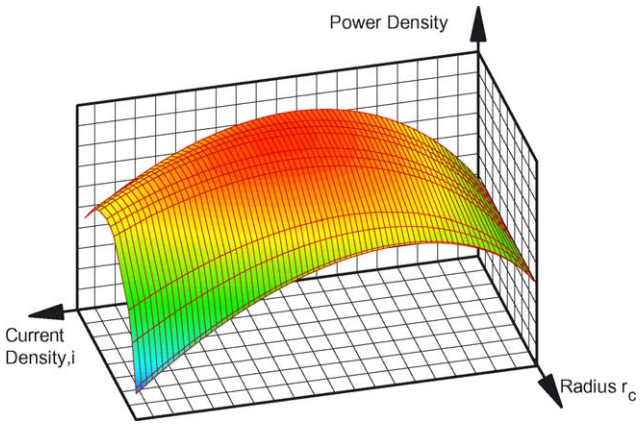

Fig. 3. Effect of the current collector size to the power density in a control area in radius of r_0 at different current densities.

When the current density increases to a certain high level, concentration polarization starts to dominate the overpotential and a severe drop of the cell voltage occurs. This results in decrease of output power in a fuel cell. In the optimization computation, the concentration-related term in electromotive force, EMF, is not considered. Therefore, the maximum power obtained in the computation virtually reflects the asymptotic power output in the fuel cell. To ensure that the comparison is on the same basis, the potential drop resulted by concentration polarization may be assumed the same for all the studied cases due to the same kind of structure of gas distributors despite the difference in the dimensions of the current collectors and their control area.

From the above consideration, the EMF for computation is set as 0.918 V ($=\Delta G^0/2F$) in all computed cases based on the assumption that the operating temperature of the SOFC is at 1000 °C. The estimation of the activation polarization for both anode side and cathode side is based on the following equation [14]:

$$\eta^{\mathrm{Act}} = \frac{RT}{F} \sinh^{-1}\left(\frac{i}{i_0}\right) \quad (5)$$

where R is the ideal gas constant, F the Faraday's constant, T the operating temperature of the fuel cell and i_0 the exchange current density, which is 6000 A m^{-2} for cathode and 3000 A m^{-2} for anode.

The computation has considered 10 groups of cases different in current-collecting area, ranging from radius of r_0 = 1.5 mm to r_0 = 10 mm. In each group, there were 11 different cases with radius of r_c varying between zero to r_0 for the cylindrical current collector. For the 11 cases in each group, at fixed r_0, the cell voltage and power density were obtained when the current density increases. For each group of cases at fixed r_0, a power density contour in the same scenario shown in Fig. 3 can be obtained and a maximum power density can be found. Corresponding to the maximum power density in each group of cases is the optimal size of current collector at the specific control area in radius of r_0. By comparing the results of the optimal performance obtained from each group

Table 1
Thickness and resistivity of components (T = 1000 °C)

	Thickness δ(μm)	Resistivity ρ_e (Ω cm)
Anode	700	0.001
Electrolyte	10	10
Cathode	50	0.013

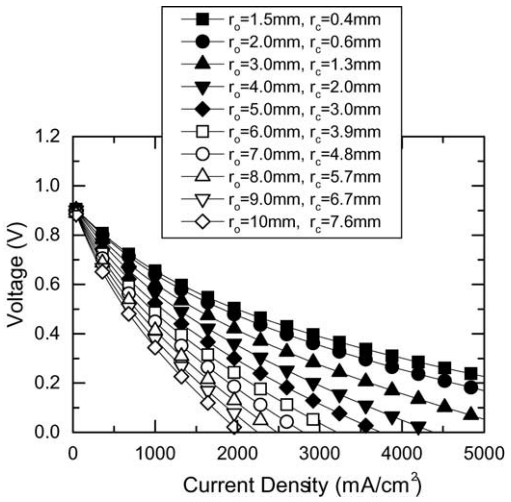

Fig. 4. Cell voltages vs. current densities at different match of the current collector and control area.

of cases, the only fully optimized match of r_0–r_c can be obtained.

Fig. 4 shows the curves of cell voltage versus current density where every curve shows the optimal performance of the optimized r_c at a fixed r_0. Due to the different match of the dimensions of current collector and its control area, the cell voltage performance is significantly different from one optimized case to another. Of all the cases, the case in smallest control area, r_0 = 1.5 mm, and an optimal current collector, r_c = 0.4 mm, is the most favorable, fully optimized match.

Corresponding to Fig. 4, the curves of power density against current density are shown in Fig. 5. The case in the smallest control area, r_0 = 1.5 mm, and an optimal current collector, r_c = 0.4 mm, can have a maximum power density four times of that from the case of r_0 = 10 mm and an optimal current collector of r_c = 7.6 mm. The optimized maximum

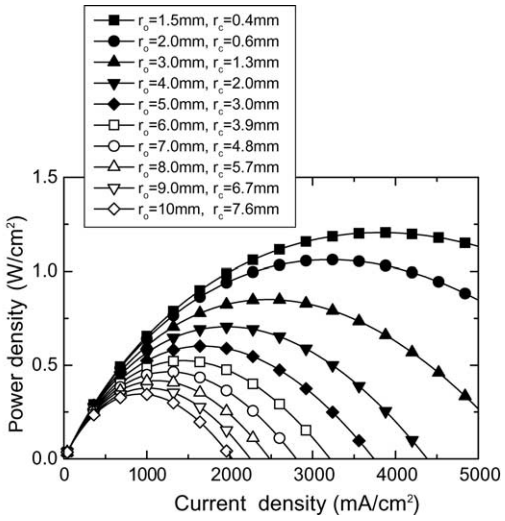

Fig. 5. Power densities vs. current densities at different match of the current collector and control area.

power density here for SOFC is higher than that of the state-of-the-art SOFCs [15–17].

For the case the control area by a current collector is small, the minimization of the current collector is more effective to maximize the total current and the output power from the control area around the current collector. Virtually a small control area around a current collector means a dense distribution of current collectors. The ohmic loss is low in such a case.

When a larger control area by a current collector is adopted, the current collectors are distributed sparsely. In such a case, when minimizing the size of current collector for maximizing the reactive area, the ohmic loss due to long current pathway will offset the effect of current maximization. Therefore, the power density cannot approach the values obtained with small control area by a small current collector. As a conclusion from Fig. 5, a small current-collecting area by a small current collector shows advantage of obtaining a high power density in a fuel cell.

4. Experimental test for PEM fuel cells

4.1. Experimental setup

The performance of the new gas distributors with cubic protruding elements was studied through a test of single PEM fuel cells and cell stacks. The proposed gas distributors were conveniently manufactured through modification of conventional gas distributor as shown in Fig. 6. In order to compare the performance of conventional and novel gas distributors, some commercially available fuel cells and cell stacks using conventional gas flow fields were tested as baseline. By interrupting the channel walls of gas distributors of baseline fuel cells, protruding cubic elements on the gas flow plates were fabricated as shown in Fig. 7. Using the same MEAs and diffusion layers from the commercial products, fuel cells having novel gas distributors were prepared.

The commercially available PEM fuel cells have MEA sheets, each with an area of 4.16 cm × 4.16 cm. In every fuel cell stack, four sheets of MEA were included to form a 4-cell stack in a serial electrical connection. All the gas distributors were made of graphite, which could be machined easily to obtain the novel structure for the current-collecting elements.

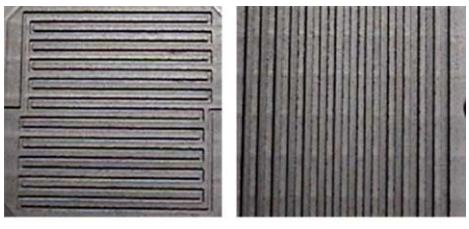

Fig. 6. Structure of baseline gas distributors for PEM fuel cells.

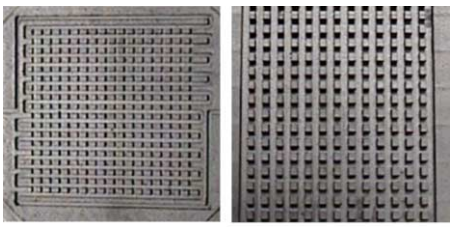

Fig. 7. Novel gas distributors for PEM fuel cells with protruding elements located in gas flow field.

The hydrogen fuel gas has a high purity to 99.999%. Impurity gases of water vapor, nitrogen, oxygen and hydrocarbons are less than 2, 5, 1 and 1 ppm, respectively. In the fuel cell stack, the fuel flows serially from one cell to another. The air is fed in parallel mode, meaning, each cell in the stack is fed with air separately. There is no external humidification to the hydrogen, and therefore the fuel cells operate with relatively low proton conductivity [18]. The depleted fuel gas from the fuel cell or cell stack is delivered to ambient air through an exit tube merged in a water bath. The released waste fuel gas bubbles, less than one per second, can be monitored. The pressure of the hydrogen gas in fuel cell is about 1.05×10^5 Pa, which is only slightly higher than ambient air pressure.

The test was conducted in an air-conditioned laboratory of about 23 °C, and the room air in laboratory was used on the cathode side through free convection mode, or forced-convection mode, depending on the setting of experimental conditions of interest. The oxygen and nitrogen molar fraction in air was estimated as 21% versus 79%, and the air pressure was 1.0 atm (1.013×10^5 Pa) or slightly higher when a small fan was used to feed air into the air channels.

A fuel cell test stand was used in the experiment, which was installed with control valves, and adjustable resistors as the external load for fuel cells. The fuel cell operating conditions were set through the control of the load resistances and the flow rates of hydrogen and air. The fuel cell output current and terminal voltage were monitored separately by two multimeters simultaneously. The output power was then obtained by multiplying the current and voltage. To avoid overheating of the fuel cells, a pair of thermocouples was located in the margin area of a graphite gas distributor for monitoring the fuel cell temperature.

The uncertainty in voltage measurement is less than 0.5% if a voltage reading is higher than 0.5 V. For electric current, when a reading is higher than 1.0 A, the uncertainty of measurement is less than 2.5%. Correspondingly, for an electrical power higher than 0.5 W, the uncertainty in measurement is less than 3%. The current densities of single cells and cell stacks are all based on the same active area of membrane of the same MEAs.

4.2. Experimental results and discussion

Figs. 8 and 9 show the curves of voltage against current density for both single fuel cells and cell stacks with gas distributors of different structures. Due to the limitation of the test system, the single cell in novel structured gas distributors could not be tested with higher current and lower voltage because a very small resistor or load was not available.

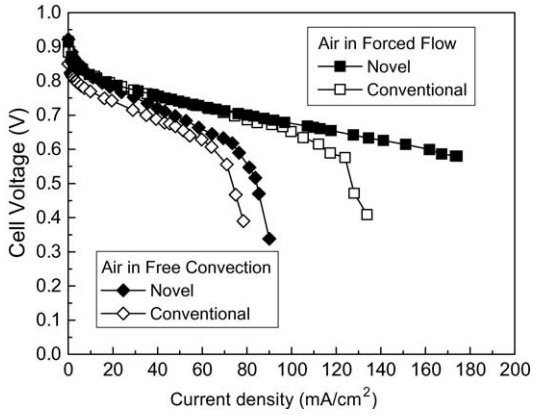

Fig. 8. Single cell voltage vs. current density.

With the increasing current density, a drop of the cell voltage at the beginning, as seen in Figs. 8 and 9, is mainly due to the activation polarization. The ohmic loss is linearly proportional to the cell current density, which contributes to the gradual drop of the cell voltage when the cell current density further increases. Along with the increase of current density, a significant drop of the cell voltage eventually occurs, which makes the fuel cell voltage too low to have any more increase of electrical power. Shown in Figs. 10 and 11 is the scenario that the output electrical powers start to drop at the current densities, where the large drop of the cell/stack voltage also happens as illustrated in Figs. 8 and 9, correspondingly. The large drop of the cell voltage is due to severe concentration polarization from deteriorating mass transport in the fuel cell.

When the sharp drop of the cell voltage is postponed to occur at higher current density, the output of electrical power of a fuel cell can be improved. This is seen in Figs. 8 and 10 as well as in Figs. 9 and 11. The different air convection mode,

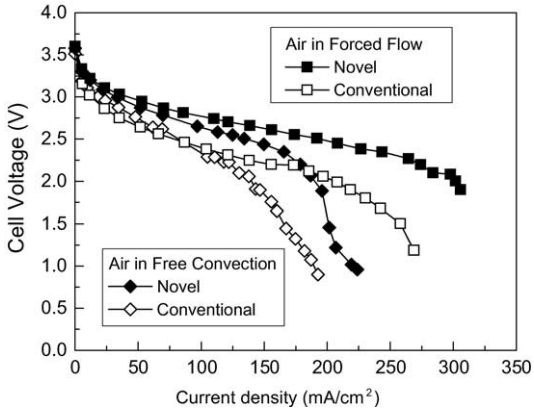

Fig. 9. Stack (four cells) voltage vs. current density. (In the forced-convection case, higher flow rate of air was fed to the cell stack with conventional gas distributors.)

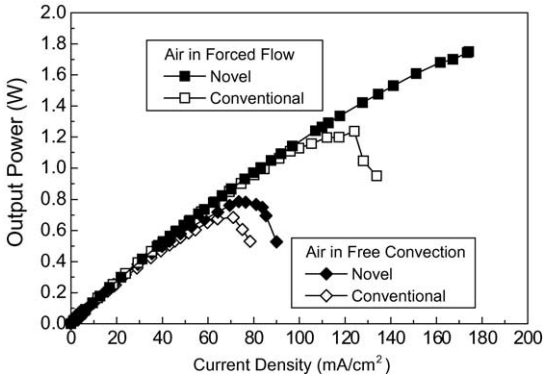

Fig. 10. Single cell output power vs. current density.

a free convection or a forced convection, makes the sharp drop of the cell voltage occur at different current densities. Obviously, the concentration polarization under a forced-convection mode is smaller than that of a free convection mode. This is the reason that the sharp drop of the cell voltage is postponed in the forced-convection case compared to the case of free convection.

As shown both in Figs. 8 and 10, when using the gas distributors of the currently proposed novel structure, the large drop of the cell voltage is significantly postponed to occurring at higher current densities compared to that of the fuel cells using distributors in conventional structures. As a result shown in Figs. 9 and 11, the electrical power is significantly improved in fuel cells and cell stacks that use the gas distributors in the novel structure.

It is understood from the preceding discussion that severe performance deterioration of PEM fuel cells might occur due to two kinds of insufficiency of mass diffusion. One is that the flow rate of air is too small to meet the need of oxygen, like the case of free convection. Another situation is that even though the flow rate of air is sufficient to provide oxygen, the mass diffusion is too weak to diffuse enough oxygen to the reaction site or the surface of MEA. Apparently, by improving the flow rate of air, both kinds of insufficiency may be mitigated from the conventional viewpoints of mass transfer enhancement. However, this needs some extra power consumption for airflow. Alternatively, the mass transfer can also be enhanced if the novel gas distributor is used. More importantly, the new gas distributors maximize contacting area for the MEA and reacting gases. This will further result in more electrochemical reactions and higher current, which also helps to improve the output power of the fuel cell.

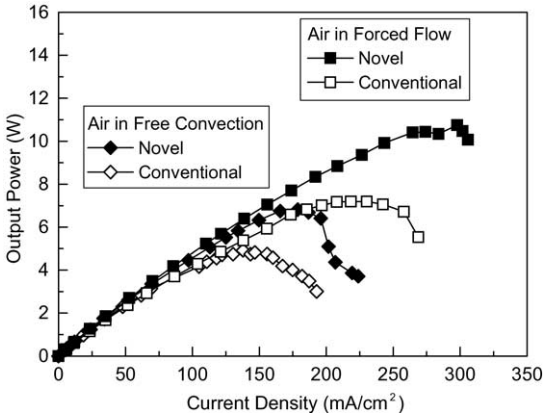

Fig. 11. Stack (four cells) power vs. current density. (In the forced-convection case, higher flow rate of air was fed to the cell stack with conventional gas distributors.)

Under a forced-convective airflow, the adoption of the novel gas distributors can improve the maximum output power by 40% for a single cell, and 50% for a cell stack compared to that of the corresponding old cell and stack as shown in Figs. 10 and 11. In the test for cell stacks with new gas distributors, a lower flow rate of air was actually used. The power consumption of the fan for airflow in the operation of the novel cell stack was 3.6 mW, which is much less than the power of 18.6 mW used for the conventional cell stack. The power consumption for the airflow takes 0.03% of the maximum output electrical power in the novel cell stack and 0.26% for the conventional cell stack. The reduction of the power consumption for the airflow might not be a significant issue if the cell stack operates at the maximum output power, but getting a higher maximum output power is certainly important because the high power density of PEM fuel cell is always desirable in practical operation.

Finally, it needs to be noted that the substantial difference of the structure of gas distributors between the currently proposed and conventional ones is the usage of the protruding elements in the novel gas distributors, which maximizes the reactive area of electrochemical reaction and enhances the mass transfer in fuel cells. The structure and alignment, or distribution, of the protruding elements are, however, open to investigation. This is because the elements are expected to implement both functions of mass transfer enhancement and current collection. For PEM fuel cells, protruding elements might also be expected to be helpful for the removal of water, or water flooding, on cathode side when humidified fuel [19,20] is used and the current density is much higher than those of the current test. Nevertheless, the optimal arrangement of protruding elements based on the discussion in this work for SOFCs and PEM fuel cells can be a very useful reference for any future work.

5. Conclusions

A novel structure of gas distributors with discretized three-dimensional current-collecting elements located in flow fields for fuel cells was proposed for the purpose of maximizing the access area of reactants to the electrode/electrolyte layer and enhancing mass transfer. The analysis model for the optimization of the distribution of three-dimensional current-collecting elements was developed.

The model was used to optimize a gas distributor for a planar-type SOFC, and optimal dimensions of the current

collector and its current-collecting area in the planar-type SOFC were obtained. It was found that a flow field distributed with relatively small current collectors surrounded by a small reactive area is preferred in order to obtain a high power density for the fuel cells.

Experimental verification test for the novel approach of gas delivery in PEM fuel cells was conducted in this work. A significant improvement of the maximum fuel cell output electrical power was obtained. Under a forced-convective airflow and non-humidified fuel, the adoption of the novel gas distributors in a PEM fuel cell can improve the maximum output power by 40% for a single cell, and 50% for a cell stack compared to that of the old cell and stack.

References

[1] S. Srinivasan, R. Mosdale, P. Stevens, C. Yang, Rev. Energy Environ. 24 (1999) 281–328.
[2] C. Yang, P. Costamagna, S. Srinivasan, J. Benziger, A.B. Bocarsly, J. Power Sources 103 (2001) 1–9.
[3] T. Susai, A. Kawakami, A. Hamada, Y. Miyake, Y. Azegami, J. Power Sources 92 (2001) 131–138.
[4] H.I. Lee, C.H. Lee, T.Y. Oh, S.G. Choi, I.W. Park, K.K. Baek, J. Power Sources 107 (2002) 110–119.
[5] S. Um, C.Y. Wang, J. Power Sources 125 (2004) 40–51.
[6] A. Kazim, H.T. Liu, P. Forges, J. Appl. Electrochem. 29 (1999) 1409–1416.
[7] P.W. Li, M.K. Chyu, J. Power Sources 124 (2003) 487–498.
[8] A. Hirano, M. Suzuki, M. Ippommatsu, Electrochem. Soc. 139 (10) (1992) 2744–2751.
[9] S. Dutta, S. Shimpalee, J.W. Vanzee, J. Appl. Electrochem. 30 (2000) 135–146.
[10] H. Dohle, A.A. Kornyshev, A.A. Kulikovsky, J. Mergel, D. Stolten, Electrochem. Commun. 3 (2001) 73–80.
[11] T.V. Nguyen, J. Electrochem. Soc. 143 (5) (1996) L103–L105.
[12] P.W. Li, S.P. Chen, M.K. Chyu, in: R.K. Shah, S.G. Kandlikar (Eds.), Proceedings of the ASME Fuel Cell Science, Engineering and Technology—2004, FUELCELL2004-2521, 2001, pp. 561–565.
[13] M.K. Chyu, Y.C. Hsing, V. Natarajan, Proceedings of the 1996 International Gas Turbine and Aeroengine Congress and Exhibition, Birmingham, UK No. 96-GT-201, 1996.
[14] S.H. Chan, K.A. Khor, Z.T. Xia, J. Power Sources 93 (2001) 130–140.
[15] Y.S. Yoo, H.K. Seo, K.S. Ahn, J.M. Oh, J.M. Bae, in: R.K. Shah, S.G. Kandlikar (Eds.), ASME Fuel Cell Science, Engineering and Technology—2004, FUELCELL2004-2449, 2004, pp. 39–43.
[16] Y.S. Amaha, H.K. Seo, K.S. Ahn, J.M. Oh, J.M. Bae, in: R.K. Shah, S.G. Kandlikar (Eds.), ASME Fuel Cell Science, Engineering and Technology—2004, FUELCELL2004-2449, 2004, pp. 39–43.
[17] J.M. Bae, J.W. Park, H.C. Lim, K.S. Ahn, Y.S. Yoo, in: R.K. Shah, S.G. Kandlikar (Eds.), ASME Fuel Cell Science, Engineering and Technology—2004, FUELCELL2004-2451, 2004, pp. 39–52.
[18] F.N. Buchi, S. Srinivasan, J. Electrochem. Soc. 144 (8) (1997) 2767–2772.
[19] T.J.P. Freire, E.R. Gonzalez, J. Electroanal. Chem. 503 (2001) 57–68.
[20] T.F. Fuller, J. Newman, J. Electrochem. Soc. 140 (5) (1993) 1218–1225.